Proceedings of the 11th World Congress on Mechanical, Chemical, and Material Engineering (MCM'25)

Barcelona, Spain -Paris, France - August, 2025

Paper No. ICCPE 148 DOI: 10.11159/iccpe25.148

Improving Separation Efficiency through Optimization of Weir Curvature in FWKO

HyunSu Jeong¹, Hwan-Gyo Kim¹, Dong-Hyun Kim¹, Ho-jin Choi¹, Youn-Jea Kim^{2†}

¹Graduate School of Mechanical Engineering, Sungkyunkwan University
2066 Seobu-ro, Suwon 16419, Republic of Korea
bb6315@g.skku.edu; ghksry3602@g.skku.edu; samechord@g.skku.edu; zatfire@g.skku.edu;
²School of Mechanical Engineering, Sungkyunkwan University
2066 Seobu-ro, Suwon 16419, Republic of Korea
yjkim@skku.edu

Abstract - The FWKO (Free Water Knockout) is the most critical component in the oil sands processing system, responsible for separating water, oil, and gas. Many studies have attempted to improve the separation efficiency by modifying the shape of the weir, which is one of the key components of the FWKO. Unlike previous studies, this research applied a concave weir based on considerations to better understand the interface and increase residence time. However, excessive curvature was found to reduce residence time, highlighting the necessity of identifying an optimal curvature for the concave weir. Using a genetic algorithm, the optimal curvature was successfully determined. As a result, the separation efficiency improved by 1.21 %p compared to the referenced model, demonstrating significant potential contributions to the oil sands industry.

Keywords: FWKO, Oil sands, Multiphase flow, Computational fluid dynamics

1. Introduction

Although the demand for petroleum resources is constantly increasing, it cannot be met solely by existing methods. As a result, non-traditional oil production technologies have gained attention, with oil sand plants becoming particularly notable due to the steady increase in potential crude oil reserves and mining volumes. Oil sands can be mined using the SAGD (Steam Assisted Gravity Drainage) method because they are buried deep underground in a high-viscosity state. The SAGD process involves injecting hot steam into the oil sands to lower their viscosity, making extraction feasible. After extraction, the resulting emulsion must be separated into water and oil. This is achieved using a FWKO unit, an oil-water separator that operates on the principles of density difference and gravity sedimentation. The basic principle of an FWKO is that the incoming bitumen enters the vessel and resides for a certain period, allowing the separation of water and oil. The oil, which accumulates at the top, then flows over the weir.

The main factors determining the separation performance of the FWKO are the residence time, the water-oil interface area, the density difference between the two fluids and the presence or absence of slugging flow. etc. Improving the separation efficiency of an FWKO without altering the inlet conditions or operating environment of the incoming bitumen is primarily limited to two factors: increasing the residence time and expanding the interface area. These shape modifications can enhance the separation process by allowing more time for phase separation and providing a larger surface for improved separation efficiency. Jung and Kim (1) numerically analyzed the separation performance of the oil-water separator based on the angle of the weir, while Yang et al. (2) examined the effects of changes in the shape of the upper part of the weir and oil viscosity on separation performance. Many previous studies have increased separation efficiency by adjusting the shape of the weir to increase the interface area, but there has been little discussion on how to increase the residence time.

In previous studies, the residence time of unseparated bitumen was considered by investigating the air-oil interface to understand the distribution of bitumen. It was found that the concentration of unseparated bitumen was higher near the walls at the air-oil interface. Based on these findings, a comparative analysis of various weir shapes revealed that concave weirs achieved higher separation efficiency. Additionally, a parametric study was conducted to observe the changes in separation efficiency depending on the curvature of the weir. The study indicated that excessive curvature increased the flow velocity, reducing residence time. It was also emphasized that there is a trade-off between the flow velocity and circulation intensity,

highlighting the need to select an appropriate weir curvature. Building upon these prior studies, the present research aims to optimize weirs with various curvatures and analyze the sensitivity of separation efficiency to changes in curvature.

2. Numerical Analysis

2.1. 3-phases separator model

In this study, a horizontal FWKO was considered as the analysis model, as shown in Fig. 1. Compared to vertical FWKO systems, horizontal FWKOs provide longer residence times, resulting in higher separation efficiency. To further enhance separation efficiency, the system is equipped with perforated baffles and a dish-head type inlet device. These components help reduce the kinetic energy of the incoming mixture, allowing for extended residence time and improved separation performance. The pressure vessel has a length of L=1.63 m and a diameter of D=0.3328 m.

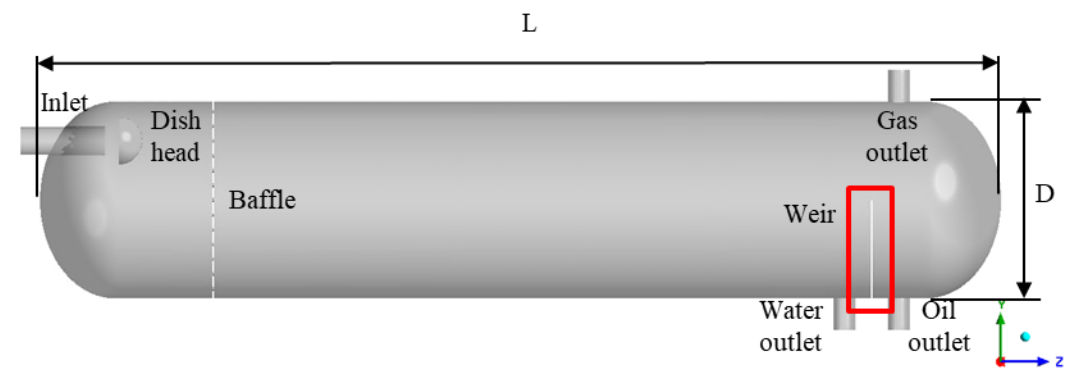


Fig. 1: Schematic of the modelled FWKO vessel.

In Fig. 1, the boxed area represents the weir. In this study, numerical simulations were conducted using the commercial software ANSYS FLUENT 2023R1 by applying a concave curvature to the top of the weir where the mixture passes through, considering various scenarios. Eq. (1) represents the ellipse equation, while Eq. (2) expresses the curvature κ as a function of position. As indicated by these equations, the curvature at each point on the ellipse is determined by the major and minor axes of the ellipse.

$$\frac{x^2}{R^2} + \frac{y^2}{r^2} = 1$$

$$\kappa = \frac{r^2 \cdot R^2}{(R^2 y^2 + r^2 x^2)^{3/2}}$$
(1)

$$\kappa = \frac{r^2 \cdot R^2}{(R^2 y^2 + r^2 x^2)^{3/2}} \tag{2}$$

Therefore, to determine the optimal curvature of the concave weir, an elliptical shape was applied to the weir design. The weir shape was created by positioning an ellipse with a major axis radius of R and a minor axis radius of r such that it is tangent to the flat top of the weir. The ellipse was then trimmed at the intersection points with the pressure vessel wall. As a result, the height of the weir increased near the vessel walls, as shown in Fig. 2.

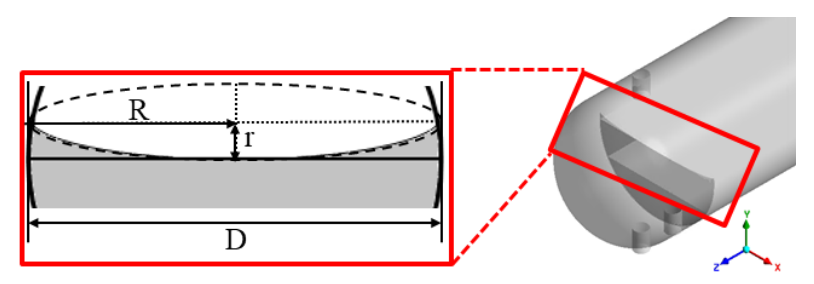


Fig. 2: Geometry of weir configuration.

The mesh used in the analysis is shown in Fig. 3. As seen in the figure, a high concentration of mesh elements is applied around the perforated baffle and the air-oil interface. To accurately capture the separation efficiency changes based on the weir shape, a dense mesh was also applied in the vicinity of the weir. The total number of mesh elements was determined to be 1.6 million based on a Grid Dependency Test (GDT), the results of which are presented in Fig. 3. The minimum orthogonal quality is 0.3, and the maximum skewness is 0.85, ensuring the mesh quality is suitable for accurate numerical analysis.

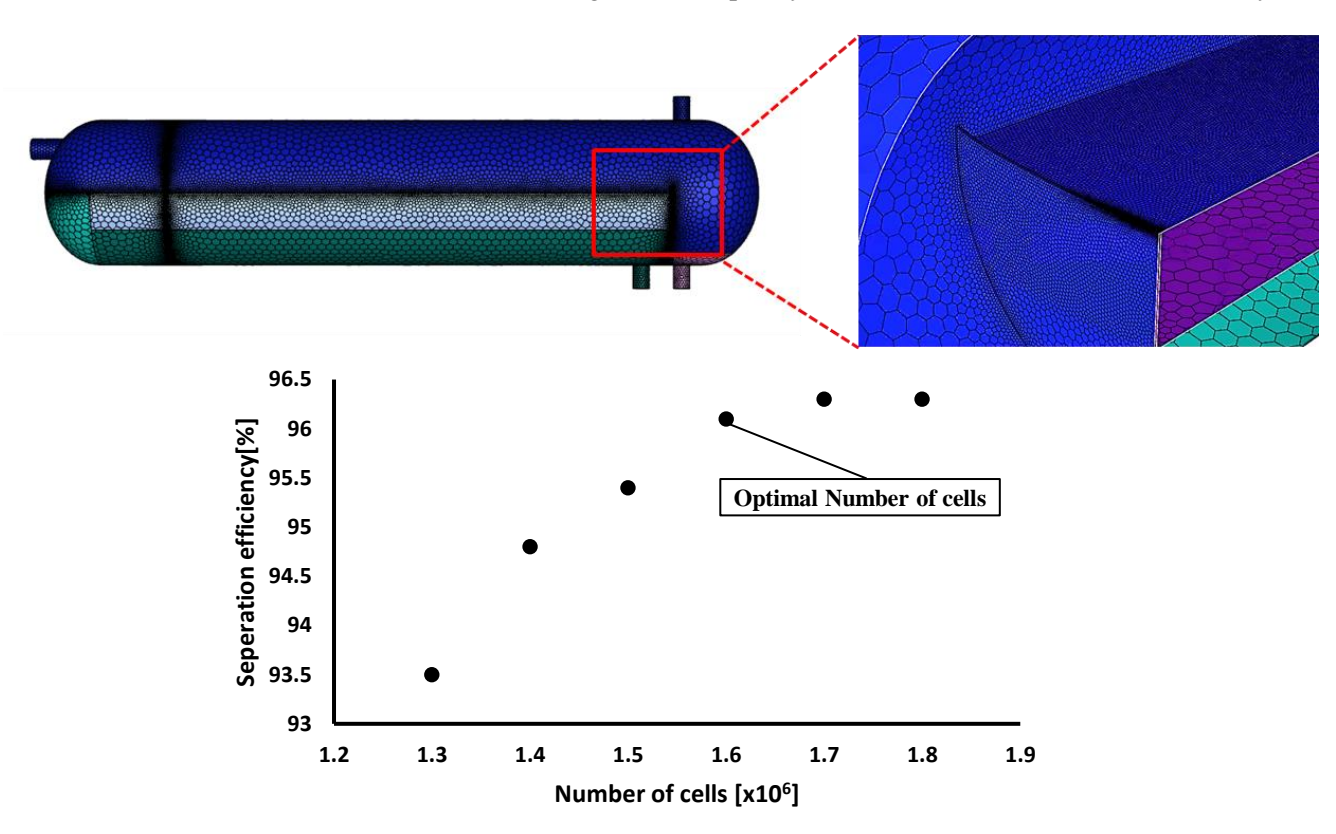


Fig. 3: Mesh and the result of grid dependency test.

2.2. Governing equations

In this analysis, the realizable k- ε model, one of the turbulence models, was employed. For multiphase flow modeling, the Volume of Fluid (VOF) method based on the Eulerian-Eulerian approach was utilized. Eq. (3) to (7) represent the governing equations used in the numerical analysis.

The continuity equation for each phase q is expressed as follows:

$$\frac{\partial}{\partial t} (\alpha_q \rho_q) + \nabla \cdot (\alpha_q \rho_q \mathbf{v}_q k) = 0 \tag{3}$$

Here, α_q represents the volume fraction of phase q, ρ_q represents the density of phase q, and \mathbf{v}_q represents the vector of phase q.

The momentum equation for each phase is expressed as follows:

$$\frac{\partial}{\partial t} (\alpha_q \rho_q \mathbf{v}_q) + \nabla \cdot (\alpha_q \rho_q \mathbf{v}_q \mathbf{v}_q) = -\alpha_q \nabla \mathbf{p} + \nabla \cdot (\alpha_q \tau_q) + \alpha_q \rho_q \mathbf{g} + \mathbf{F}_q \tag{4}$$

Here, p represents the pressure, τ_q represents the viscous stress tensor, **g** represents the gravitational acceleration, and \mathbf{F}_q represents the interphase interaction force.

The surface tension model is considered as an additional term in the VOF method, and the surface tension term can be expressed as follows:

$$\mathbf{F}_{surface} = \sigma \kappa' \nabla \alpha_q \tag{5}$$

Here, σ represents the surface tension coefficient, and κ' represents the curvature.

In the realizable k- ε model, the equations for the turbulent kinetic energy (k) and the turbulent dissipation rate (ε) are given as follows:

$$\frac{\partial}{\partial t}(\rho k) + \nabla \cdot (\rho k \mathbf{v}) = \nabla \cdot \left(\frac{\mu_t}{\sigma_k} \nabla k\right) + G_k + G_b - \rho \varepsilon \tag{6}$$

$$\frac{\partial}{\partial t}(\rho\varepsilon) + \nabla \cdot (\rho\varepsilon\mathbf{v}) = \nabla \cdot \left(\frac{\mu_t}{\sigma_{\varepsilon}}\nabla\varepsilon\right) + C_1 S_{\varepsilon} - C_2 \rho \frac{\varepsilon^2}{k + \sqrt{\nu\varepsilon}}$$
(7)

Here, μ_t represents the turbulent viscosity coefficient, G_k represents the turbulence energy production term, G_b represents the buoyancy term, σ_k and σ_{ε} are empirical turbulence model constants, C_1 and C_2 are empirical coefficients, and S represents the magnitude of the strain rate tensor.

In multiphase flow using the VOF (Volume of Fluid) method, the equation for tracking the volume fraction is expressed as follows:

$$\frac{\partial \alpha_q}{\partial t} + \mathbf{v} \cdot \nabla \alpha_q = 0 \tag{8}$$

2.3. Boundary conditions

The FWKO system receives a mixture of water, oil, and air at the inlet, and each phase is discharged through its respective outlet. The physical properties of each phase are presented in Table 1.

Phase	Density [kg/m^3]	Viscosity [Pa·s]	Surface tension [<i>N</i> / <i>m</i>]
Gas	1.225	1.7894×10 ⁻⁵	-
Oil	830	0.1	0.027 (with gas)
Water	998.2	0.001003	0.072 (with gas)
			0.04 (with oil)

Table 1: Material properties.

At the inlet, the flow rate was calculated and set to satisfy 60 BPD(barrel/day) with an SOR(steam to oil ratio) of 2.2. The air outlet was set to a gauge pressure of 0, while the oil and water outlets were assigned a constant static pressure to simulate the effect of valves used in actual FWKO systems to maintain the interface height. According to Behin and Azimi (3), the highest separation efficiency is achieved when the oil interface height is set to half of the vessel diameter, and this condition was applied accordingly. The detailed values are presented in Table 2.

ВС	Phase	Variable	Value
Inlet	Mixture Velocity		0.31056m/s
	Gas	Gauge pressure	0
Outlet	Oil	Static pressure	677.44Pa
	Water	Static pressure	1983.78Pa

Table 2: Boundary conditions.

For the initial conditions, patches were applied to ensure faster convergence. The water region was set from the bottom up to half the height of the weir, while the oil region was defined immediately above the water region, extending up to the full height of the weir.

3. Optimization

In this study, ANSYS DesignXplorer 2023R1 was used to analyze the separation efficiency based on curvature. As shown in Fig.2 the minor axis radius r, which determines the height near the vessel wall, and the major axis radius R, which defines the curvature, were set as shape variables. Before proceeding with the optimization, a reference model was analyzed by setting R to half of the FWKO vessel's diameter (0.1664 m) and the minor axis radius to 0.02 m. Numerical simulations were conducted to observe the flow behavior within the FWKO over a duration of 800 seconds. The separation efficiency (η) was evaluated by averaging the separation efficiency values from 700 to 800 seconds, as defined in Eq. (9). In this equation, N represents the number of time steps between 700 and 800 seconds, \dot{m}_{oil} denotes the oil mass flow rate at the oil outlet and \dot{m}_{H_2O} represents the water mass flow rate at the oil outlet. The separation efficiency of the reference model was found to be 96.13%.

$$\eta = \frac{1}{N} \sum_{t=700}^{800} \frac{\dot{m}_{oil}}{\left(\dot{m}_{oil} + \dot{m}_{H_2O}\right)} \tag{9}$$

3.1. Design of experiment (DOE)

Next, a Design of Experiments (DOE) study was conducted to identify the correlation between the design variables R and r and the separation efficiency, as well as to derive an optimal design point. The DOE type selected was Latin Hypercube Sampling (LHS) design, and the sample type used was Central Composite Design (CCD) Samples. The LHS method is particularly useful in cases where experimental costs are high or computational simulations are expensive. Compared to traditional grid-based sampling methods, it provides a more uniform distribution with fewer samples, enabling efficient experimental planning. The CCD-based experimental design follows Eq. (10), where the number of experiments y is determined by the number of shape variables k'. Based on the reference values of R=0.1664 m and r=0.02 m, a total of 9 design variable combinations were generated. However, since R cannot be smaller than the FWKO vessel radius of 0.1664 m, a constraint condition was applied accordingly.

$$y = 2^{k'} + 2k' + 1 \tag{10}$$

Table 3: Design points of DOE and results at the design points.

Case	<i>R</i> [m]	r [m]	η
1	0.18167	0.016667	0.9646
2	0.19167	0.025556	0.9653
3	0.17167	0.012222	0.9537
4	0.18833	0.03	0.9460
5	0.175	0.043333	0.9515
6	0.19833	0.021111	0.9590
7	0.185	0.047778	0.9348
8	0.195	0.038889	0.9486
9	0.17833	0.034444	0.9567

3.2. Response surface method

The Response Surface Methodology (RSM) technique approximates the relationship between separation efficiency and design variables using data obtained from numerical simulations. One of the RSM techniques, Non-parametric regression (NPR), is a method that utilizes kernel functions to estimate values based on local information of the data. This technique is advantageous as it smoothly connects data points and is useful for predicting function values at specific locations. Therefore, NPR was employed in the optimization process of this study. The graph shown in Fig. 4 presents the predicted values obtained through NPR on the y-axis and the observed values from numerical simulations on the y-axis. The fact that the output values are closely aligned along the diagonal line demonstrates the reliability of the NPR technique in this analysis.

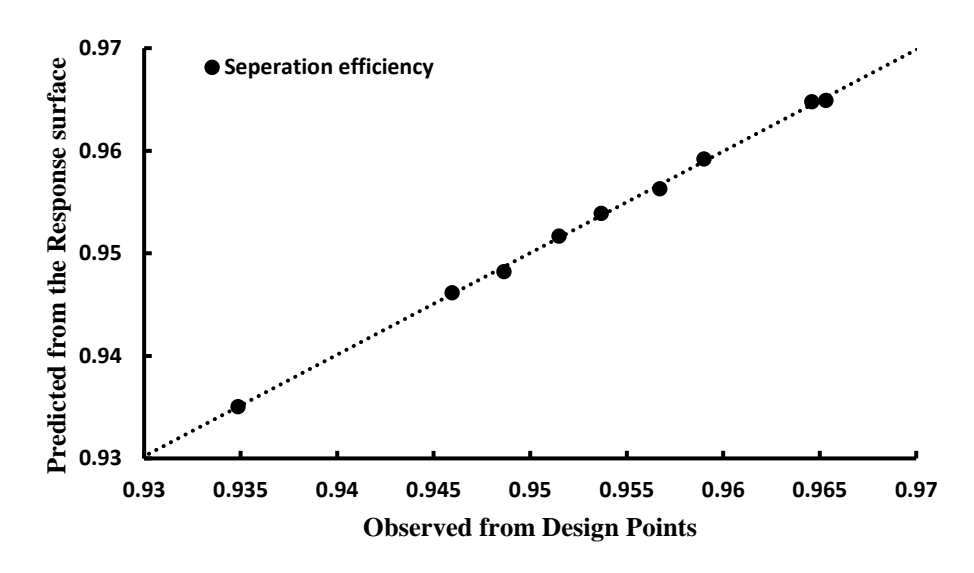


Fig. 4: Comparison of the predicted value and the observed value.

Additionally, the quantitative indicators related to reliability further confirmed the accuracy of the analysis. The coefficient of determination (R^2) was calculated to be 0.999 (with the best value being 1), and the root mean square error (RMSE) was found to be 0.0003 (with the best value being 0), reaffirming the reliability of the NPR method.

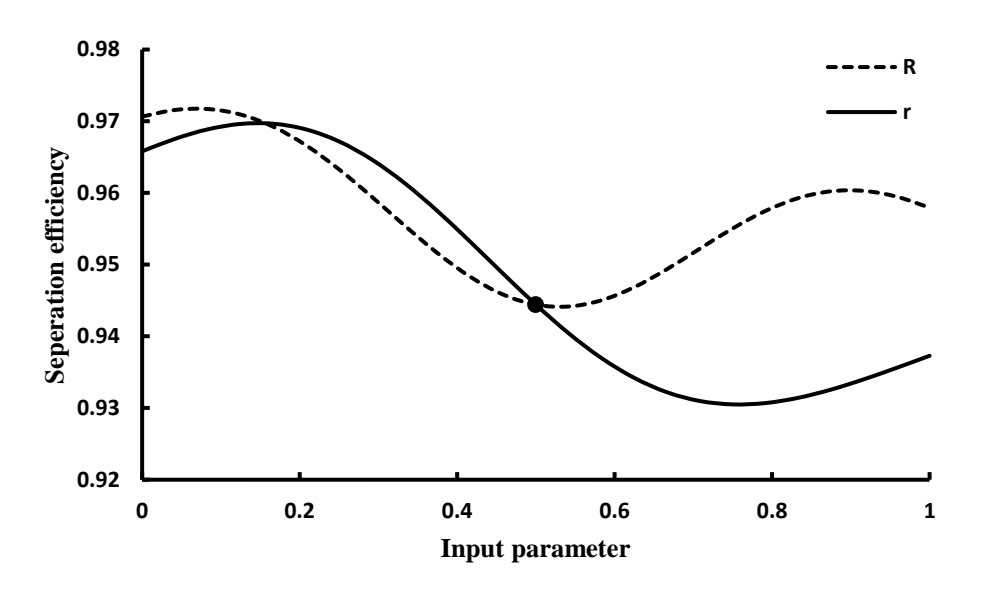


Fig. 5: Local sensitivity analysis results.

A sensitivity analysis was conducted using NPR, and the results are presented in Fig. 5. In Fig. 5, the horizontal axis represents the ratio of each input parameter within its respective range, while the vertical axis represents the separation efficiency. As described earlier in Section 3.1, R cannot be smaller than the radius of the FWKO vessel. Therefore, the dashed line representing R shows meaningful values when the ratio is above 0.5, with an initial decrease followed by an increase. Similarly, the value of r exhibits a decreasing trend initially and then increases. Both design variables exhibit complex curves rather than simple linear relationships with the output parameter. Based on these results, it can be inferred that the optimal value for R lies above the reference model value of 0.1664 m, while the optimal value for r is smaller than the reference model value of 0.02 m.

3.3. Genetic algorithm

In the final step, the weir shape was optimized using screening, a method within the genetic algorithm framework. The objective was to maximize separation efficiency, with the constraints set as η <1 and r,R<0.1664. As a result of the optimization, the predicted optimal values for r and R were found to be 0.017333 m and 0.19032 m, respectively, with the expected separation efficiency reaching 97.51%. To validate the optimization results, numerical simulations were conducted under optimized conditions. The simulation results yielded a separation efficiency of 97.34%, showing a minimal error of 0.17 %p compared to the predicted value. Furthermore, the optimized model showed an improvement of 1.21 %p compared to the reference model, demonstrating the effectiveness of the optimization process.

	<i>R</i> [m]	r [m]	η	Difference	Curvature $[m^{-1}]$
Reference model	0.1664	0.02	0.9613	-	416
Optimization model	0.19032	0.017333	0.9734	+1.21%	633
Worst model (Case 7)	0.185	0.047778	0.9348	-2.65%	81

Table 4: Comparison of three models results.

Table 4 compares three models: the reference model, the optimized model, and the model with the lowest separation efficiency from the DOE results. The difference column represents the increase or decrease compared to the reference model, and the final column, Curvature, indicates the curvature at the point closest to the center of the ellipse in the weir with applied curvature. Overall, it was observed that an increase in curvature led to an improvement in separation efficiency. This is

because excessive curvature (where smaller curvature values indicate a more pronounced curve) reduced the cross-sectional area at the top of the weir, accelerating the flow. Fig. 6 presents contours of the velocity passing through the top of the weir for each model, with the gray area representing the weir. As shown in the figure, the lowest efficiency was observed in Case 7, where a high velocity was detected. Finally, to confirm the effectiveness of applying curvature to the weir, Case 3, which had the highest curvature (least pronounced curve) among the DOE cases, was examined. In Case 3, the curvature was $1149 \ [m^{-1}]$, and the separation efficiency achieved was 95.37%. This result suggests that simply increasing the curvature does not always lead to higher separation efficiency; however, applying an appropriate curvature to the weir does have a positive impact on performance.

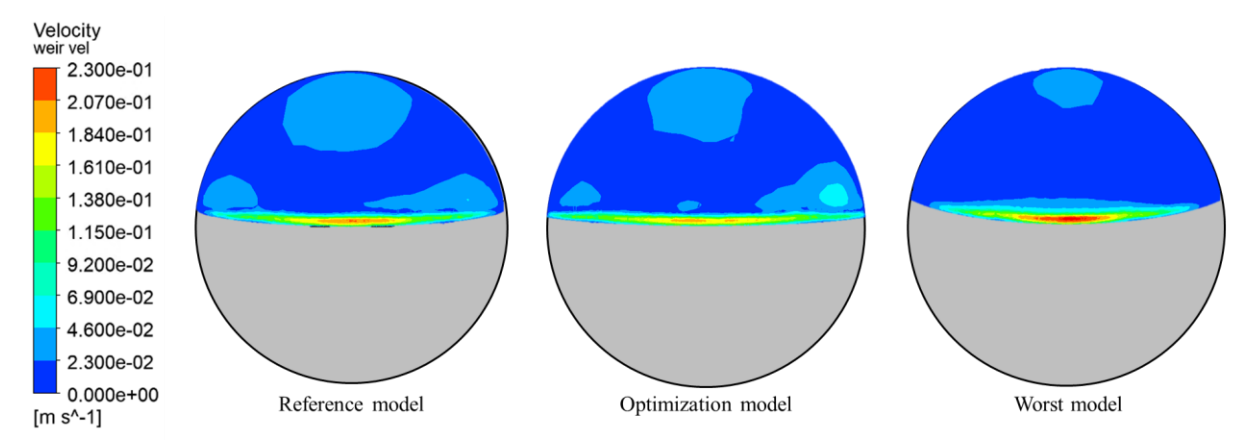


Fig. 6: Comparison of velocity contours for three models.

4. Conclusion

Based on previous studies that suggested concave weirs improve separation efficiency by inducing swirling flow of the mixture near the vessel walls, this study examined the impact of weir curvature on separation efficiency. The design variables considered were the major and minor axis radii of the ellipse, denoted as R and r, respectively. Using LHS, a DOE approach, nine design points were derived. Sensitivity analysis and optimization of the input parameters were conducted using NPR and screening techniques to identify the optimal design point. As a result of the optimization, the optimized model achieved a 1.21 %p improvement in separation efficiency compared to the reference model, and a 3.86 %p improvement compared to the least efficient design point. It was observed that separation efficiency is highly sensitive to curvature, displaying a complex relationship rather than a simple linear trend. The findings suggest that separation efficiency is influenced by a combination of factors, including the degree of swirling flow and flow velocity, rather than by curvature alone in a straightforward manner.

Acknowledgement

This research was supported by the Korea Agency for Infrastructure Technology Advancement (KAIA) grant funded by the Ministry of Land, Infrastructure, and Transport, grant number (RS-2022-00142936).

References

- [1] Jung, K.J. and Kim, Y.J., "Effect of Weir Configurations on the Performance of Oil-Water Separator," *International Journal of Fluid Machinery and Systems*, 2020, 13(4): p. 759-766.
- [2] Yang, H.J., Kang, H.S., Kim, Y.J., "The effect on the performance of FWKO by changing the configuration of weir and the viscosity of oil," *The KSFM Journal of Fluid Machinery*, 2024, Vol. 27, No. 1, pp. 110~115.
- [3] Behin, J. and S. Azimi, "Experimental and computational analysis on influence of water level on oil-water separator efficiency.", *Separation Science and Technology*, 2015, 50(11): p. 1695-1700.